Metamorphic evolution of Precambrian basement in the southern Ruby Range, southwestern Montana

Martin A. Cramer, Brennus Voarino, and Julie A. Baldwin

Department of Geosciences, University of Montana, Missoula, MT 59812

Introduction

The Ruby Range records key aspects of the assembly and stabilization of the Laurentian craton (Figure 1) from the Archean to the Paleoproterozoic. Two major periods of tectonothermal activity have been documented within the basement exposures of southwestern Montana (Figure 2): 1) a ~1780 Ma metamorphic event, the Big Sky orogeny, that may record ocean basin closure and continent-continent collision and 2) a more cryptic metamorphic event at ~2500 Ma that may be related to rift activity or an older tectonic event. Preliminary pressure-temperature modeling of the ~1780 Ma event suggests upper amphibolite facies metamorphism between 700-850° C and 7.5-10 kbar. Additionally, while historically considered entirely reworked Archean cratonic lithosphere, recent evidence suggests that the Ruby Range may include accreted Proterozoic lithosphere and/or passive margin sediments (O'Neill and Christiansen, 2002; Alcock and Muller, 2012).

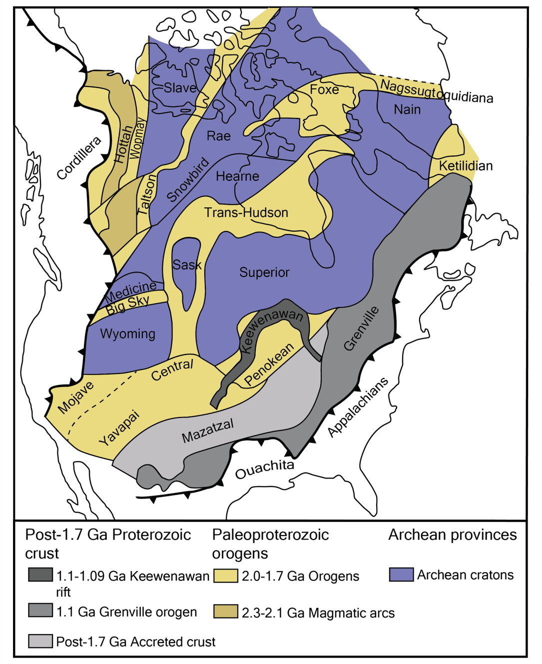

Figure 1. The North American craton, Laurentia, with Archean cratons and Proterozoic orogens. Modified after Hoffman (1988), Bleeker and Hall (2007), and Harms (2011).

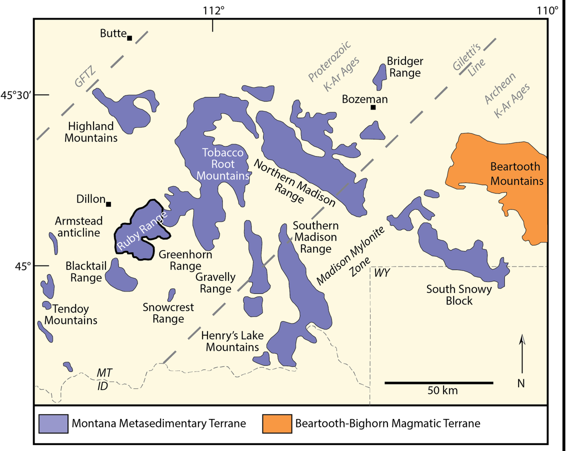

Figure 2. Laramide uplifts of the northwest margin of the Wyoming province, with the Ruby Rang outlined in black. GFTZ = Great Falls Tectonic Zone (after Mogk et al., 1992).

Hypothesis

The Ruby Range represents a mid-crustal window during continental assembly at ~1800 Ma that will aid us in understanding Proterozoic crustal reactivation and growth at the western margin of Laurentia.

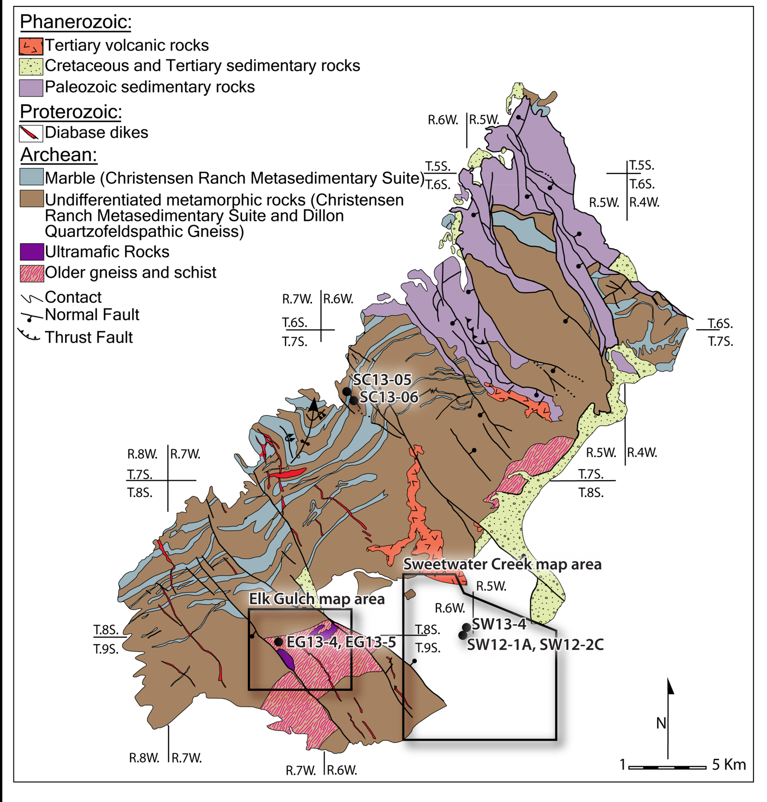

Figure 3. Geologic map of the Ruby Range, with study areas and sample locations annotated. Modified after Karasevich (1981) and Jones

Objectives

- Place constraints on the timing of metamorphism during the Big Sky orogeny within the Ruby Range.
- Determine if units within the Ruby Range have a shared or distinct metamorphic history prior to the Big Sky orogeny.
- Use trends in REE concentrations over time to describe the growth and breakdown of garnet and feldspar.

Methods

- The scanning electron microscope (SEM) was used for *in situ* location and characterization of monazite. Monazite was located using the backscattered electron detector (BSE) and compositional grain maps were collected using the energy dispersive spectroscopy (EDS) detector.
- Petrochronologic data was gathered *in situ* from monazite using the laser ablation split stream inductively coupled plasma mass spectrometry (LASS-ICPMS) facilities of the University of California, Santa Barbara (Kylander-Clark et al., 2013).
- Individual LASS-ICPMS analyses were conducted using a 10 µm spot size and a 26 second acquisition time for simultaneous analysis of U-Th-Pb isotope and rare earth element (REE) concentrations from the same sample volume.
- U-Th-Pb isotope concentrations were collected using a Nu Plasma HR multi-collector ICPMS (MC-ICPMS). REE concentrations were collected using a Agilent 7700 quadrupole ICPMS.

Geologic maps

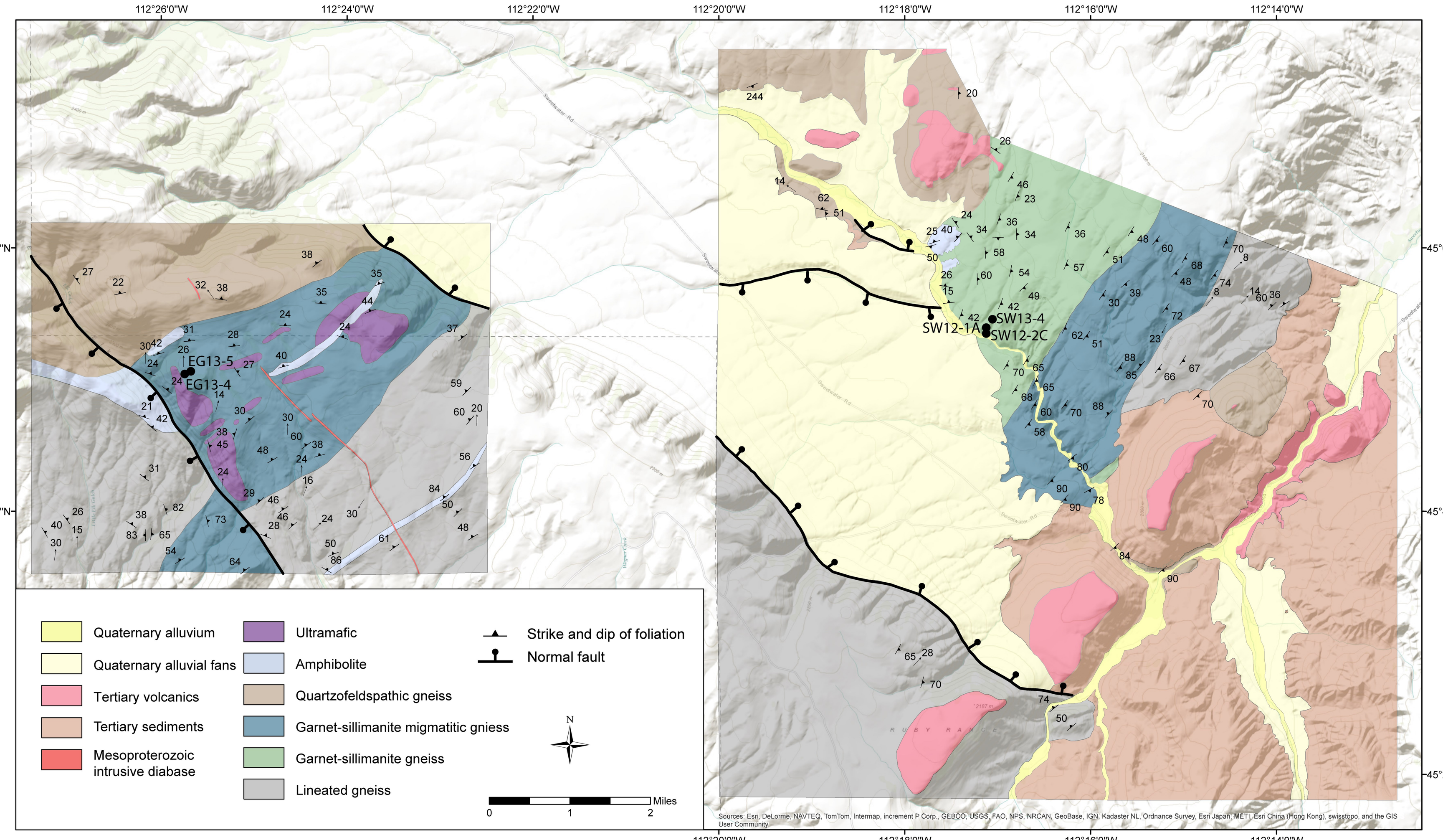

Figure 4. Geologic maps of the Elk Gulch (left) and Sweetwater (right) areas. The quartzofeldspathic unit includes minor garnet bearing layers. The garnet-sillimanite migmatitic gneiss unit is dominated by migmatitic metapelitic rocks. In the Sweetwater area the unit includes a higher proportion of migmatitic quartzofeldspathic gneiss and in the Elk Gulch area there are minor layers of garnet-sillimanite orthoamphibolite. The garnet-sillimanite gneiss unit is defined by the presence of significant metapelitic lithologies, including garnet-sillimanite-cordierite gneisses. Pelitic layers range in thickness from less than 1 m to 3 m, with individual sillimanite porphyroblasts up to 5 cm long. The lineated gneiss unit is defined by the presence of a strongly lineated quartzofeldspathic gneiss, with minor migmatitic rocks. Amphibolite occurs throughout all of the units, as well as ultramafics, leucogneiss, and garnet bearing leucogneiss.

Petrology

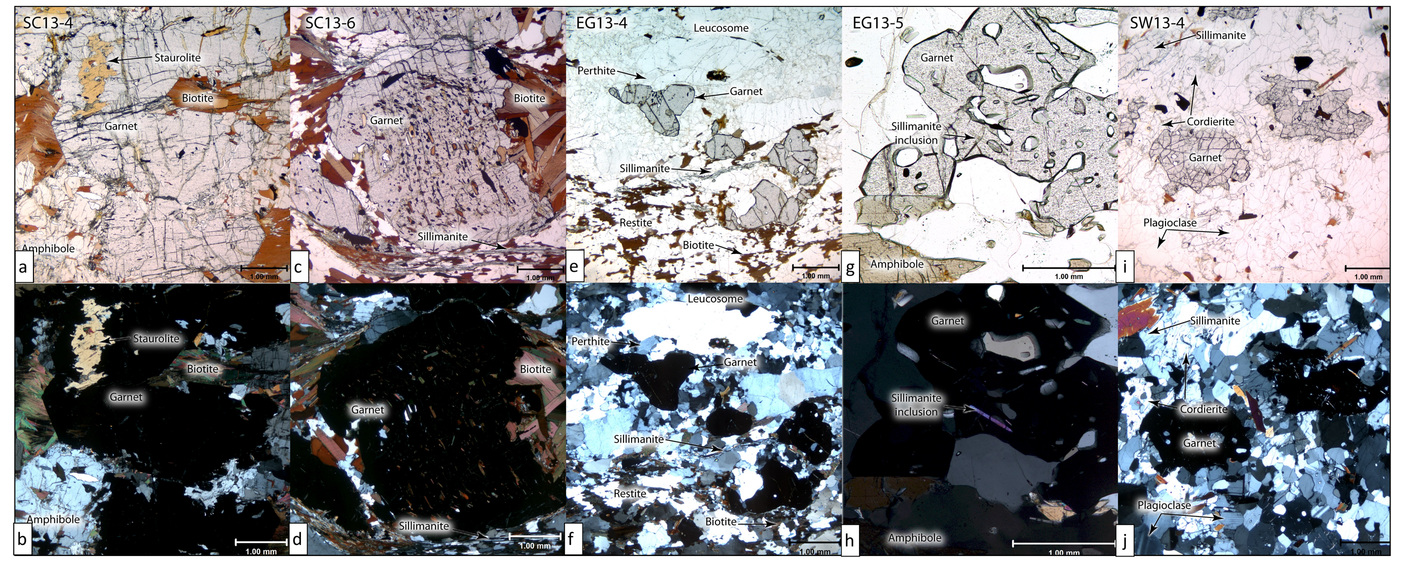

Figure 5. Photomicrographs of investigated samples. Sample SC13-4 is a garnet-staurolite orthoamphibolite with staurolite often occurring as inclusions within garnet (a & b). Sample SC13-6 is a garnet-sillimanite gneiss, garnets have abundant synkinematic inclusion trails and sillimanite occurs as prismatic needles in matrix (c & d). EG13-4 is a garnet-sillimanite migmatitic gniess. Garnet and sillimanite are present throughout the leucosome and restite, feldspar exists as perthite (e & f). EG13-5 is a garnet-sillimanite-cordierite orthoamphibolite, with cordierreplacing garnet (g & h). SW13-4 is a garnet-sillimanite-cordierite gneiss. Cordierite is found replacing garnet and as an abundant matrix mineral (i & j). Samples SW12-1A & SW12-2C are also both garnet-sillimanite-cordierite gneisses, but with less abundant cordierite than sample SW13-4. Additionally, samples SW12-1A and SW12-2C have large cm scale sillimanite lathes (k).

SEM analysis

Figure 6. EDS compositional maps of monazite showing Y zoning (a). Compositional domains often correspond to age domains and guide analysis spot selection. BSE images of petrographic setting (b).

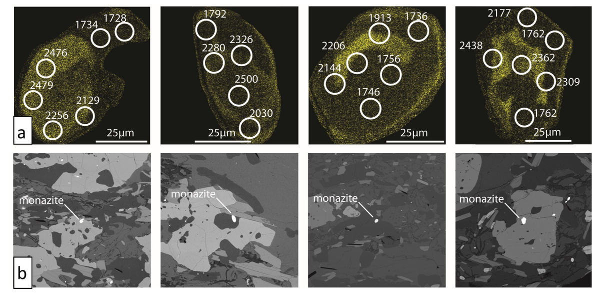

Petrochronology

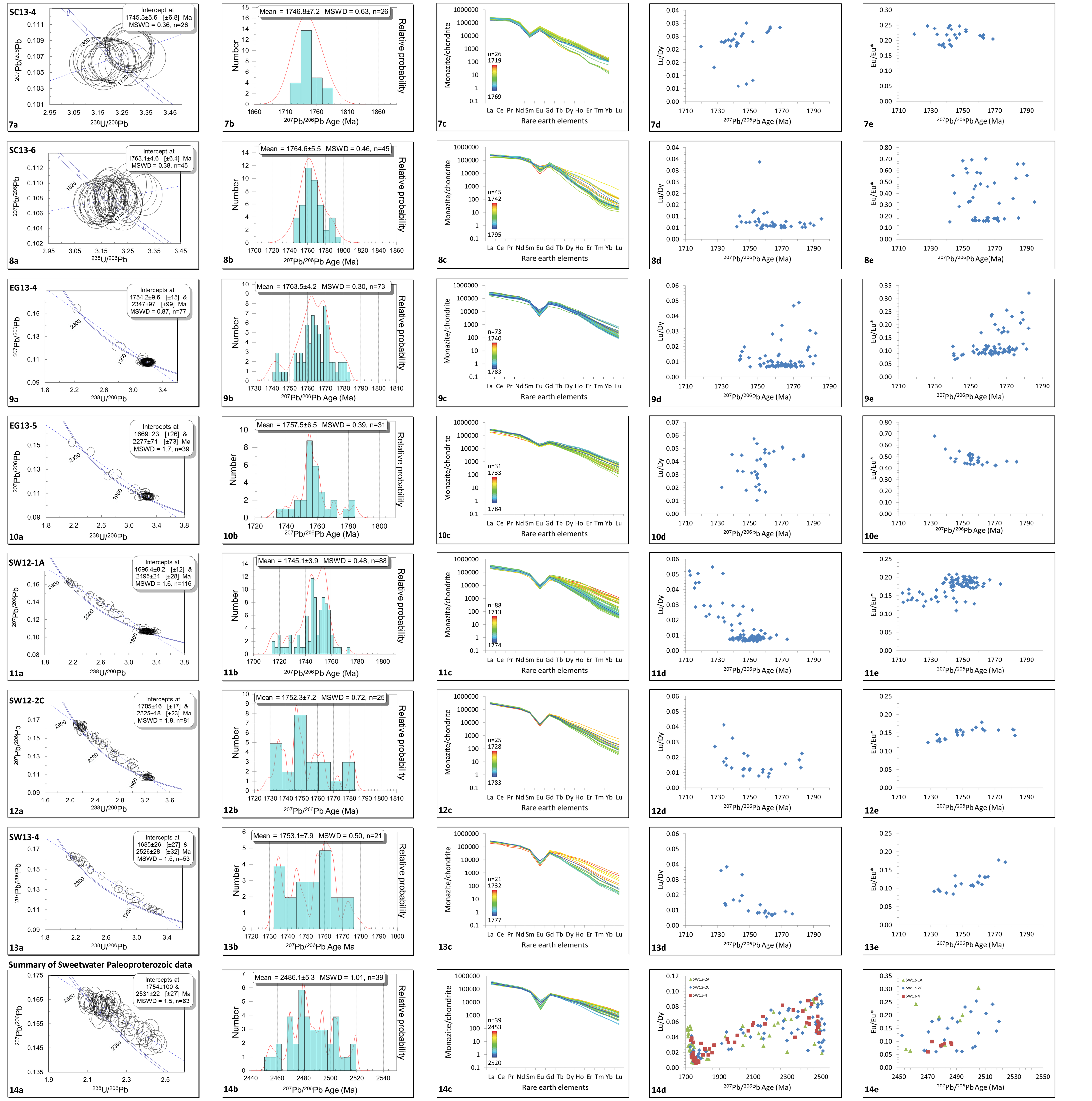

Figures 7-14. U-Pb isotope and REE data. Figures 7-13 correspond to individual samples and present data related to the ~1780 Ma event. Figure 14 represents the amalgamated data from samples SW12-1A, SW12-2C, and SW13-4 for the ~2500 Ma event. Columns correspond to diagram type: Tera-Wasserburg concordia diagrams for all analyses (a), probability density plots with mean age (b), chondrite normalized diagrams of REE compositions of monazite color coded by age (c), chondrite normalized Lu-Dy ratio plotted vs $^{207}Pb/^{206}Pb$ Age (d), chondrite normalized Eu anomaly $(Eu/(\sqrt{Sm^*Gd}))$ plotted vs $^{207}Pb/^{206}Pb$ Age (e). Columns b-e present data for concordant analyses only, with 14d an exception, in order to highlight the effect of mixed domain analysis on measured REE concentrations.

Interpretations

- Prior to ca. 1780 Ma, the Stone Creek, Elk Gulch, and Sweetwater areas had different metamorphic histories (Figures 7-13a).
- The Stone Creek samples bear no monazite ages older than the ca. 1780 Ma event (Figures 7 & 8). This implies that the Christensen Ranch Metasedimentary Suite (Figure 2) is primarily a Proterozoic metasediment sequence, and not Archean as previously assumed.
- The Elk Gulch migmatitic sample EG13-5 shows an increase in Eu/Eu* from ca. 1770 Ma, implying feldspar breakdown.
- Sweetwater samples all show a significant increase in Lu/Dy from ca. 1765-1710 Ma, implying garnet breakdown during retrograde metamorphism (Figures 11d-13d).
- Similarly, Sweetwater samples all show a decrease in Eu/Eu* from ca. 1765-1710 Ma, implying feldspar growth during retrograde metamorphism (Figure 11e-13e).
- Sweetwater samples show elevated heavy REE concentrations (Figure 14d) from 2530-2450 Ma event. This is interpreted as the initial metamorphism of the Sweetwater garnet-sillimanite gneiss unit that did not reach garnet forming conditions (Figure 14).
- Eu anomalies for the ca. 2530 Ma event do not differ significantly from the Eu anomalies in the ca. 1780 Ma event (Figures 11e-14e), implying that by the onset of monazite growth during the older event, feldspar had already formed. Additionally, Eu/Eu* shows a decrease from ca. 2530-2450 Ma , implying continued feldspar growth.

Conclusions

In situ petrochronology of monazite provides new insights into the metamorphic evolution of rocks in the Ruby Range. These data suggest the juxtaposition of previously unrelated Archean and possibly Proterozoic crust during the ca. 1780 Ma Big Sky orogeny. These data also provide insight into a regional cryptic ca. 2530 Ma tectonometamorphic event. Changing REE concentrations in monazite over time document the formation and breakdown of garnet and feldspar. Future work will integrate these results with phase equilibria modeling to define the pressure-temperature-time paths of metamorphism within the Ruby Range.

Acknowledgements

This research is supported by the Tobacco Root Geological Society Jack Harrison Scholarship, the Wyoming Geological Association David Love Scholarship, and the Colorado Scientific Society Student Research Grant. Thanks to Andrew Kylander-Clark with the University of California, Santa Barbara campus, LASS-ICPMS facilities.

References

Alcock, J., and Muller, P., 2012, A Paleoproterozoic sedimentary basin within the Wyoming craton exposed in the Ruby Range, SW Montana: Identified by field relations and geochronology: Northwest Geology, v. 41, p. 47-62.

Bleeker, W., and Hall, B., 2007, The Slave Craton: Geology and metallogenic evolution, in Goodfellow, W.D., ed., Mineral Deposits of Canada: A Synthesis of Major Deposit-Types, District Metallogeny, the Evolution of Geological Provinces, and Exploration Methods: Geological Association of Canada, Mineral Deposits Division, Special Publication No. 5, p. 849-879.

Harms, T.A., Brady, J.B., and Cheney, J.T., 2011, Exploring the Proterozoic Big Sky orogeny in southwest Montana, in, Varga, R.J. and Kadyk, D.: Keck Geology Consortium Proceedings of the Twenty-Fourth Annual Keck Research Symposium in Geology, p. 59-64.

Hoffman, P.F., 1988, United plates of America, the birth of a craton: Early Proterozoic assembly and growth of Laurentia: Annual Review of Earth and Planetary Science, v. 16, p. 543-603.

Jones, C, 2008, U-Pb geochronology of monazite and zircon in Precambrian metamorphic rocks from the Ruby Range, SW Montana: Deciphering geological events that shaped the NW Wyoming province: unpublished master's thesis, Kent State University.

Karasevich, L.P., 1980, Structure of the pre-Beltian metamorphic rocks of the northern Ruby Range, southwestern Montana: unpublished master's thesis, Pennsylvania State University.

Kylander-Clark, A.R.C., Hacker, B.R., and Cottle, J.M., 2013, Laser-ablation split-stream ICP petrochronology: Chemical Geology, v. 345, p. 99-112.

Mogk, D.W., Mueller, P.A., and Wooden, J.L., 1992, The nature of Archean terrane boundaries: an example from the northern Wyoming province: Precambrian Research, v. 55, no. 1-4, p. 155-168.

O'Neill, J.M., Christiansen, R.L., 2002, Geologic map of the Hebgen Lake 30 by 60 minute quadrangle, Beaverhead, Madison, and Gallatin counties, Montana, Park, and Teton counties, Wyoming, and Clark and Fremont counties, Idaho: Montana Bureau of Mines and Geology.